

Impaired Recycling of Apolipoprotein E4 Is Associated with Intracellular Cholesterol Accumulation*

Received for publication, August 13, 2004, and in revised form, October 7, 2004
Published, JBC Papers in Press, October 12, 2004, DOI 10.1074/jbc.M409324200

Joerg Heeren^{‡§¶}, Thomas Grewal^{||}, Alexander Laatsch^{‡**}, Nils Becker[‡], Franz Rinninger^{‡‡},
Kerry-Anne Rye^{§§}, and Ulrike Beisiegel[‡]

From the [‡]Institute for Biochemistry and Molecular Biology II: Molecular Cell Biology and ^{‡‡}Department of Internal Medicine, University Hospital Eppendorf, D-20246 Hamburg, Germany, ^{||}Centre for Immunology, St. Vincent's Hospital, University of New South Wales, Darlinghurst, New South Wales 2010, Australia, and ^{§§}Heart Research Institute, Camperdown, Sydney, New South Wales 2050, Australia

After internalization of triglyceride-rich lipoproteins (TRL) in hepatoma cells, TRL particles are immediately disintegrated in the early endosomal compartment. This involves the targeting of lipids and apoprotein B along the degradative pathway and the recycling of TRL-derived apoE through recycling endosomes. Re-secretion of apoE is accompanied by the concomitant association of apoE and cellular cholesterol with high-density lipoproteins (HDL). Since epidemiological data showed that apoE3 and apoE4 have differential effects on HDL metabolism, we investigated whether the intracellular processing of TRL-derived apoE4 differs from apoE3-TRL. In this study, we demonstrated by radioactive and immunofluorescence uptake experiments that cell-surface binding and internalization of TRL-derived apoE4 are increased compared with apoE3 in hepatoma cells. Pulse-chase experiments revealed that HDL-induced recycling, but not disintegration and degradation, of apoE4-enriched TRL is strongly reduced in these cells. Furthermore, impaired HDL-induced apoE4 recycling is associated with reduced cholesterol efflux. Studies performed in Tangier fibroblasts showed that apoE recycling does not depend on ATP-binding cassette transporter A1 activity. These studies provide initial evidence that impaired recycling of apoE4 could interfere with intracellular cholesterol transport and contribute to the pathophysiological lipoprotein profile observed in apoE4 homozygotes.

Intestinal chylomicrons and liver-derived very low-density lipoproteins (VLDL)¹ represent triglyceride-rich lipoproteins

* This work was supported by the Deutsche Forschungsgemeinschaft Research Grants HE 3645/2-1, Be 829/5-1, Gr 258/10-2, Ri 436/8-1, the GRK 366 "Molecular Endocrinology and Metabolism," and the Gretl Raymond Foundation (to T. G.). The costs of publication of this article were defrayed in part by the payment of page charges. This article must therefore be hereby marked "advertisement" in accordance with 18 U.S.C. Section 1734 solely to indicate this fact.

§ Both authors contributed equally to this work.

¶ To whom correspondence should be addressed: IBM II: Molecular Cell Biology, University Hospital Eppendorf, Martinistrasse 52, D-20246 Hamburg, Germany. Tel.: 49-40-42803-3917; Fax: 49-40-42803-4592; E-mail: heeren@uke.uni-hamburg.de.

** Supported by a fellowship from the Studienstiftung des Deutschen Volkes.

¹ The abbreviations used are: VLDL, very low-density lipoproteins; apo, apoprotein; ABCA1, ATP-binding cassette transporter A1; BSA, bovine serum albumin; Chol, cholesterol; DiI, 1,1'-dioctadecyl-3,3',3'-tetramethylindocarbocyanine; HDL, high-density lipoproteins; HuH7, human hepatoma cell line 7; LDL, low-density lipoproteins; OH-Chol, 22(R)-hydroxycholesterol; TRL, triglyceride-rich lipoproteins; PBS, phosphate-buffered saline; RA, 9-cis-retinoic acid; DMEM, Dulbecco's

(TRL) that deliver lipids and lipophilic vitamins to other cells of the body. Lipoprotein lipase-mediated hydrolysis of TRL at the luminal side of endothelial cells resulted in the formation of TRL remnants, which are rapidly cleared by the liver (for review see Refs. 1 and 2). Lipoprotein lipase remained associated with these remnants, which simultaneously became enriched with high-density lipoprotein (HDL)-derived apoprotein E (apoE). Both lipoprotein lipase and apoE then facilitated the internalization of TRL remnants via the LDL receptor-related protein 1 and the low-density lipoprotein receptor (3–7).

After receptor-mediated endocytosis, the intracellular processing of TRL is very complex. We and others (8–12) demonstrated that TRL is disintegrated in peripheral endosomes, which is followed by a differential sorting of TRL components. In human hepatoma cells and fibroblasts, the majority of TRL lipids is targeted to the lysosomal compartment, whereas TRL-derived apoE is found in peripheral recycling endosomes (9, 10). Subsequently, substantial amounts of TRL-derived apoE are recycled back to the cell-surface, re-secreted (9), and found associated with newly synthesized or exogenous lipoproteins (10, 11, 13, 14). We recently discovered that HDL stimulates and serves as an acceptor for recycled apoE in hepatocytes *in vitro* and *in vivo* (10, 13). This new link between TRL-derived apoE and HDL metabolism is associated with cholesterol efflux and involves the internalization of HDL particles to preexisting endosomes containing TRL-derived apoE (13).

ApoE has many different functions in the metabolism of lipids and lipoproteins. Besides its role in the clearance of TRL-remnants (6), apoE very effectively stimulates cholesterol efflux from macrophages (15–17) and is involved in hepatic lipoprotein assembly (18, 19). ApoE exists in three isoforms, which differ at two positions in the protein (apoE2, Cys¹¹² and Cys¹⁵⁸; apoE3, Cys¹¹² and Arg¹⁵⁸; and apoE4, Arg¹¹² and Arg¹⁵⁸). These variations resulted in different metabolic properties of apoE isoforms, which are linked to an increased risk for the development of atherosclerosis and Alzheimer's disease (20, 21). ApoE2 exhibits strongly reduced binding affinity to heparan sulfate proteoglycans and the LDL receptor (22). This results in the accumulation of remnant particles in plasma and most probably contributes to the observed association of apoE2 with familial type III hyperlipoproteinemia (23). ApoE4 correlates with high plasma LDL cholesterol levels and is associated with atherosclerosis and Alzheimer's disease (20, 21). However, despite the importance of apoE4 as a risk factor, the cellular mechanisms, which are responsible for the differences between apoE3 and apoE4, are yet unclear. The binding of apoE4 to

modified Eagle's medium; GAPDH, glyceraldehyde-3-phosphate dehydrogenase; MES, 4-morpholineethanesulfonic acid.

lipoprotein receptors and clearance of TRL remnants are comparable or even higher in comparison with apoE3 (24–27). Thus, the dissimilar behavior of apoE isoforms on the intracellular metabolism of apoproteins and lipids could contribute to the development of disease. Compared with apoE3, apoE4 is less efficient in promoting cholesterol efflux in fibroblasts and astrocytes (28, 29), indicating that apoE isoforms differentially affect the mobilization of cellular cholesterol. Therefore, we investigated whether there are potential differences in the intracellular processing of internalized TRL-derived apoE3 and apoE4 that could explain these findings. In this study, we demonstrated that HDL-induced recycling, but not internalization, degradation, or disintegration of TRL-derived apoE4, is impaired compared with apoE3. This process does not depend on the ATP-binding cassette transporter A1 (ABCA1) activity. Most importantly, reduced apoE4 recycling is associated with a decrease in cholesterol efflux. Thus, impaired apoE4 recycling could explain the low apoE protein and cholesterol content of HDL, which is associated with the human apoE4 allele (20, 26, 30–32).

EXPERIMENTAL PROCEDURES

Antibodies and Reagents—BSA, glycine, 22(R)-hydroxycholesterol (OH-Chol), paraformaldehyde, nucleus stain Hoechst dye 33342 (4',6-diamidino-2-phenylindole) and 9-cis-retinoic acid (RA) were from Sigma. Mowiol 4-88 was purchased from Calbiochem. DMEM, PBS, fetal calf serum, trypsin, penicillin, and streptomycin were from Invitrogen. Iodogen was from Pierce. [¹²⁵I] and ³H-cholesterol were from Amersham Biosciences. Heparin (Liquemin®) was purchased from Roche Applied Science. Polyclonal antibody against human apoE was from Dako. LysoTracker and 1,1'-dioctadecyl-3,3,3',3'-tetramethylindocarbocyanine (DiI) were from Molecular Probes. Cy3- and Cy5-fluorescence protein-labeling kits were from Amersham Biosciences. Cy2-conjugated goat anti-rabbit F(ab')₂ fragments and horseradish peroxidase-conjugated goat anti-rabbit F(ab')₂ fragments were purchased from Jackson ImmunoResearch.

Cell Culture—Human hepatoma cell line 7 (HuH7) and normal and Tangier fibroblasts (33) were grown in DMEM supplemented with 10% fetal calf serum and penicillin/streptomycin at 37 °C in 5% CO₂.

Ligand Preparation and SDS-PAGE—ApoE-depleted HDL₃ (*d* = 1.125–1.21 g/ml) from normal healthy donors (34), TRL from an apoCII-deficient patient (apoE2/3), and VLDL from normolipemic blood donors (apoE3/3 and apoE4/4, respectively) were isolated as described previously (5). ApoE3 and apoE4 from human VLDL were isolated by preparative SDS-PAGE (35). Human recombinant apoE3 and apoE4 were expressed in BL21 *Escherichia coli* (constructs were provided by Dr. Karl Weisgraber, Gladstone Institute, San Francisco, CA) and purified by gel filtration chromatography (36). TRL and VLDL were radiolabeled by the iodine monochloride method. ApoE isoforms were radiolabeled with Iodogen according to the manufacturer's instructions. 100 μg of unlabeled or ¹²⁵I-labeled apoE isoforms (native and recombinant) were associated with TRL (0.5 mg of protein) to prepare apoE3-TRL, apoE4-TRL (final concentration 0.23 mg protein/ml) or ¹²⁵I-apoE3-TRL, and ¹²⁵I-apoE4-TRL (13). The protein concentrations of the ¹²⁵I-TRL and the ¹²⁵I-apoE-TRL preparations were 0.22 ± 0.1 mg/ml, whereas ¹²⁵I-VLDL was 0.41 ± 0.13 mg/ml and the specific radioactivity was 90–140 cpm/ng protein, respectively. Radiolabeling of TRL and VLDL apoproteins was confirmed by SDS-PAGE and autoradiography as described previously (10). For immunofluorescence, 100 μg of recombinant apoE3 and apoE4 were labeled with Cy3 or Cy5, associated with TRL, and re-isolated by ultracentrifugation to obtain Cy3-apoE3-TRL and Cy5-apoE4-TRL, respectively. Fluorescent label was exclusively found in apoE as determined by SDS-PAGE followed by in-gel fluorescence analysis (data not shown). Incorporation of DiI into apoE3-TRL and apoE4-TRL was performed as described previously (9). Non-incorporated DiI was removed by PD10 (Amersham Biosciences) gel chromatography. To analyze the apolipoprotein composition of TRL particles, 2–10 μg of the different lipoprotein preparations were delipidated by chloroform/methanol extraction and apoproteins were separated by SDS-PAGE on 4–12% gradient gels (NuPAGE®, Invitrogen). Apoproteins were visualized with a Coomassie Blue protein stain.

Immunofluorescence—For immunofluorescence, hepatoma cells were incubated with 5 μg/ml apoE3, apoE3-TRL, apoE4-TRL, DiI-apoE3-

TRL, or DiI-apoE4-TRL in DMEM + 2% BSA for 15–60 min at 37 °C. For uptake experiments, cells were washed in DMEM, treated with heparin at 4 °C for 5 min, and fixed in 4% paraformaldehyde. To study apoE recycling, cells were treated as above and incubated for an additional 60 min at 37 °C in DMEM (0.1% BSA) ± 50 μg/ml HDL₃ before fixation. Supernatants were harvested for subsequent Western blot analysis (see below). Indirect immunofluorescence against apoE and nuclear staining with 4',6-diamidino-2-phenylindole were performed as described previously (9). Full cell images were taken with an Axiovert 100 microscope equipped with a Zeiss AxioCam. Confocal images were collected using a Zeiss LSM 510 (version 3.0). For living cell microscopy, cells were incubated with 1 μg/ml Cy3-apoE-TRL, Cy5-apoE4-TRL, and 1 μM LysoTracker in DMEM + 2% BSA for 0–30 min at 37 °C. Confocal images were taken every minute in the multitrack mode using optimized pinhole adjustment for each fluorochrome.

Western Blotting—Hepatoma cells were incubated with TRL, apoE3-TRL, or apoE4-TRL for 60 min at 37 °C, washed, and solubilized in 50 mM Tris-HCl, pH 8.0, 2 mM CaCl₂, 80 mM NaCl, and 1% Triton X-100 for 20 min at 4 °C. After centrifugation for 15 min with 13,000 × *g* at 4 °C, supernatants were harvested and protein concentrations were determined. In another set of experiments, hepatoma cells were incubated with TRL, apoE3-TRL, or apoE4-TRL for 60 min at 37 °C, washed, and incubated for an additional 60 min at 37 °C ± 50 μg/ml HDL₃ in DMEM + 0.1% BSA. The media were harvested, filtered (0.45 μm), and cleared by centrifugation at 14,000 × *g* for 10 min. Cellular proteins (5 μg/lane) and supernatants were separated by 4–12% SDS-PAGE and 10% SDS-PAGE, respectively, and immunoblotted against apoE. After incubation with peroxidase-conjugated secondary antibodies, the reaction product was detected using the ECL system (Amersham Biosciences).

Cell Surface Binding, Uptake, Degradation, and Recycling Assays—For radioactive cell-surface binding and uptake experiments, hepatoma cells were washed with PBS and incubated with ¹²⁵I-apoE3-VLDL or ¹²⁵I-apoE4-VLDL (2.5–10 μg/ml) for 60 min at 4 °C on ice or at 37 °C in DMEM + 5% BSA, pH 7.4, respectively. Cells then were washed with ice-cold PBS. To exclusively measure internalized radioactivity in uptake experiments, cells were washed with 100 units/ml heparin to remove surface-bound material (9, 37). Finally, cells were solubilized in 0.1 N NaOH to determine the amount of cell-surface bound (4 °C) or internalized (37 °C) radioactivity. Values were normalized to total cellular protein (9). For degradation experiments, hepatoma cells were incubated with 10 μg/ml ¹²⁵I-apoE3-VLDL or ¹²⁵I-apoE4-VLDL for 60 min at 37 °C in DMEM and 5% BSA, pH 7.4. Cells were washed as described above and incubated at 37 °C for an additional 30–300 min. The media were harvested, the trichloroacetic acid-precipitable material was removed, and the amount of degraded (¹²⁵I-tyrosine) radioactivity in the supernatants was determined. Values were normalized to total cellular protein.

For pulse-chase experiments, cells were incubated with 2.5 μg/ml ¹²⁵I-TRL, ¹²⁵I-apoE3-TRL, or ¹²⁵I-apoE4-TRL, washed, and treated with heparin as described above. To promote recycling, radiolabeled cells were incubated for 60–240 min at 37 °C with DMEM + 0.1% BSA supplemented with 50 μg/ml HDL₃. The content of trichloroacetic acid-precipitable recycled radioactivity in the harvested media was then determined (9).

Reverse Transcriptase-PCR—To induce ABCA1 expression, human hepatoma cells were treated overnight with 5 mM OH-Chol and 5 mM RA (38). Total RNA was isolated, and ABCA1 mRNA levels were determined using quantitative reverse transcriptase-PCR as described previously (39). The values obtained for ABCA1 were normalized to GAPDH mRNA levels. The primers to determine ABCA1 (123-bp cDNA fragment) and GAPDH (242 bp) expression were as follows: ABCA1 (position 4522–4644; NM005502) (forward, 5'-ACTCTTAAACGCCCT-CACCAAAGAC-3'; reverse, 5'-GTCTGGGGAAGTGGGGCAGT-3'); GAPDH (position 619–860, NM002046) (forward, 5'-ACTGCCACCA-GAAGACTGT-3'; reverse, 5'-ACCACCTTCTTGATGTCATCATA-3').

Cholesterol Efflux Experiments—To achieve cholesterol loading, 100,000 cpm/ml ³H-cholesterol in ethanol were incubated with cells overnight at 37 °C as described previously (40). The cells then were washed and incubated with TRL, apoE3-TRL, or apoE4-TRL for 60 min at 37 °C. After heparin treatment (see above), cells were incubated in DMEM + 0.1% BSA in the presence or absence of 50 μg/ml HDL₃ for an additional 60 and 240 min at 37 °C. The media were harvested, and cells were lysed in 0.1 N NaOH. The amount of ³H-cholesterol in the media and cells was determined and normalized to total cellular protein content.

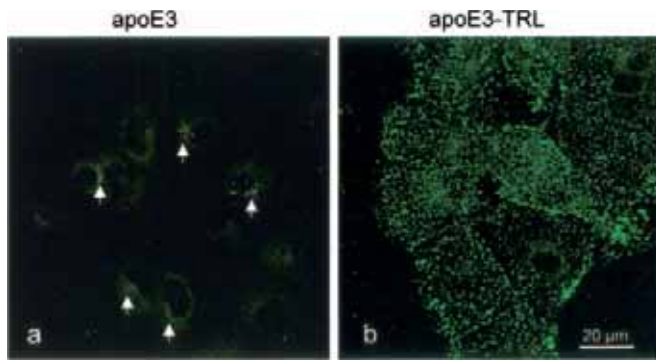


FIG. 1. Uptake of lipid-free and TRL-associated apoE3 in hepatoma cells. HuH7 hepatoma cells were incubated with (a) lipid-free apoE3 (*apoE3*) and (b) TRL-associated apoE3 (*apoE3-TRL*) for 60 min at 37 °C. After the removal of cell-bound material with heparin, cells were fixed and sections (1 μm width) were analyzed by confocal fluorescence microscopy for apoE. Arrows in *a* point to endogenous apoE staining. Bar is 20 μm.

RESULTS

Accumulation of Internalized TRL-derived ApoE4—Epidemiological studies have clearly shown that apoE3 and apoE4 isoforms have differential effects on lipoprotein metabolism. Some observations have indicated that the internalization and intracellular processing of TRL-derived apoE isoforms may help to explain the differences of apoE isoforms in lipid metabolism. The inheritance of apoE4 is associated with increased internalization of VLDL in hepatocytes but not in fibroblasts (25). These findings correlated with the enhanced plasma clearance of VLDL in apoE4 compared with apoE3 mice (27). Therefore, initial experiments addressed the effects of enhanced internalization of apoE4 on the intracellular processing of TRL-associated apoproteins. First, the internalization of lipid-free and TRL-associated apoE3 and apoE4 into hepatoma cells was compared. TRL-associated apoE3 accumulated in peripheral endosomes (Fig. 1B), whereas after incubation with lipid-free apoE3 only a weak staining was observed (Fig. 1A). This staining represents endogenous apoE in perinuclear compartments, because it was also present in cells incubated without any exogenous apoE (data not shown). Similar results were obtained with lipid-free apoE4 (data not shown). To exclude that the enrichment of TRL particles with apoE3 or apoE4 could differentially alter the overall TRL apoprotein composition, possibly affecting the internalization of apoE3-TRL and apoE4-TRL, the apoprotein composition of TRL, apoE3-TRL, and apoE4-TRL was analyzed by SDS-PAGE (Fig. 2A). Coomassie Blue staining revealed that TRL isolated from apoCII-deficient patients contained apoB₁₀₀ and apoB₄₈, indicating that both chylomicrons and VLDL were present. The other major apoproteins of native TRL were apoE and apoC (Fig. 2A, lane 1). TRL enriched with recombinant apoE3 or apoE4 contained comparable amounts of apoE3 and apoE4 (Fig. 2A, lanes 2 and 3, respectively). When higher apoprotein amounts were analyzed, similar amounts of apoB₁₀₀ and apoB₄₈ were detected in apoE3-TRL and apoE4-TRL (data not shown). We then compared the internalization of TRL-associated apoE isoforms by immunofluorescence (Fig. 2B). HuH7 hepatoma cells were incubated with TRL alone as well as with apoE3- and apoE4-enriched TRL (Fig. 2B). Enrichment of TRL with the two apoE isoforms led to a more pronounced accumulation of apoE4 in peripheral endosomes as compared with apoE3. The uptake experiments using TRL enriched with a 1:1 mixture of apoE3 and apoE4 revealed an intermediate accumulation of apoE (data not shown).

Using radiolabeled VLDL from patients homozygous for apoE3 or apoE4, similar results were obtained in radioactive

cell-surface binding (Fig. 2C) and uptake experiments (Fig. 2D), respectively. In these experiments, cell-surface binding and internalization of ¹²⁵I-apoE4-VLDL was increased 1.5–1.8-fold compared with ¹²⁵I-apoE3-VLDL. To analyze whether more efficient degradation of apoE3 could contribute to the increased accumulation of apoE4 as compared with apoE3 (Figs. 1 and 2), the degradation of internalized ¹²⁵I-apoE3-VLDL and ¹²⁵I-apoE4-VLDL in hepatoma cells was compared (Fig. 2E). Cells were loaded with radiolabeled apoE3- or apoE4-VLDL and then chased for different time periods. At each time point, the non-precipitable radioactivity relative to total internalized radioactivity was determined (Fig. 2E). Consistent with the results described above, most of the radiolabeled apoproteins escaped proteolytic degradation and only some degradation products (up to 25% after 300 min), probably derived from apoB, appeared in the media.

Taken together, higher cell-surface binding and uptake of apoE4-TRL, as opposed to apoE3-TRL, does not result in obvious changes in the intracellular distribution and degradation of internalized apoE isoforms into hepatoma cells.

ApoE4 Does Not Interfere with the Disintegration of Internalized TRL Particles—Internalized TRL are disintegrated in endosomal compartments followed by a differential sorting of TRL components. Whereas TRL-derived apoE is targeted to peripheral endosomes, most TRL lipids are directed along the lysosomal pathway (9, 10). To identify whether increased apoE4 internalization could result in a differential sorting of apoE isoforms, we first compared the localization of internalized TRL-derived apoE3 and apoE4 in the early endosomal compartment (Fig. 3A). To ensure comparability of internalized apoE isoforms, HuH7 cells were simultaneously incubated with 2 μg/ml Cy3-apoE3-TRL (*a*, in red) and 1 μg/ml Cy5-apoE4-TRL (*b*, in green) for 30 min at 37 °C. Internalized TRL-derived apoE was found in EEA1-positive endosomes under these conditions (13). The localization of apoE3 and apoE4 was then analyzed by confocal microscopy. Although apoE4 is internalized more rapidly as compared with apoE3 (Fig. 2), a similar punctate endosomal staining and co-localization of apoE isoforms were observed, indicating that both apoE isoforms are similarly trafficking through the endosomal compartment after internalization (Fig. 3A, *a–c*, arrows). Marginal co-localization of apoE3 with LysoTracker confirmed that TRL-derived Cy3-apoE3 is not targeted to the perinuclear pre-lysosomal/lysosomal compartment (Fig. 3B). Similar results were obtained with Cy5-apoE4-TRL (data not shown).

To follow the disintegration and the intracellular fate of apoE3- and apoE4-TRL-derived lipids, the fluorescent phospholipid analog, DiI, was incorporated into TRL. HuH7 cells were incubated with DiI-labeled apoE3-TRL (Fig. 4, *a–c*) and apoE4-TRL (Fig. 4, *d–f*) for 30 min at 37 °C, respectively, and the localization of apoE isoforms and DiI was studied by confocal microscopy. In agreement with previous experiments, TRL-derived apoE and lipids were disintegrated under these conditions (9). Both apoE3 and apoE4 remain in peripheral endosomes, whereas TRL lipids such as DiI are transported predominantly to the perinuclear (pre-lysosomal/lysosomal) compartment. Taken together, these findings indicated that the transport into early endosomal compartments and the disintegration of apoE3-TRL and apoE4-TRL are identical.

Impaired HDL-induced ApoE4 Recycling Is Associated with Reduced Cholesterol Efflux—We have previously demonstrated that the recycling of TRL-derived apoE from peripheral endosomes is stimulated by exogenous HDL₃ (13). To identify potential differences between the apoE isoforms on HDL₃-induced recycling of TRL-derived apoE, HuH7 cells were pre-loaded with apoE3- and apoE4-enriched TRL and re-secretion

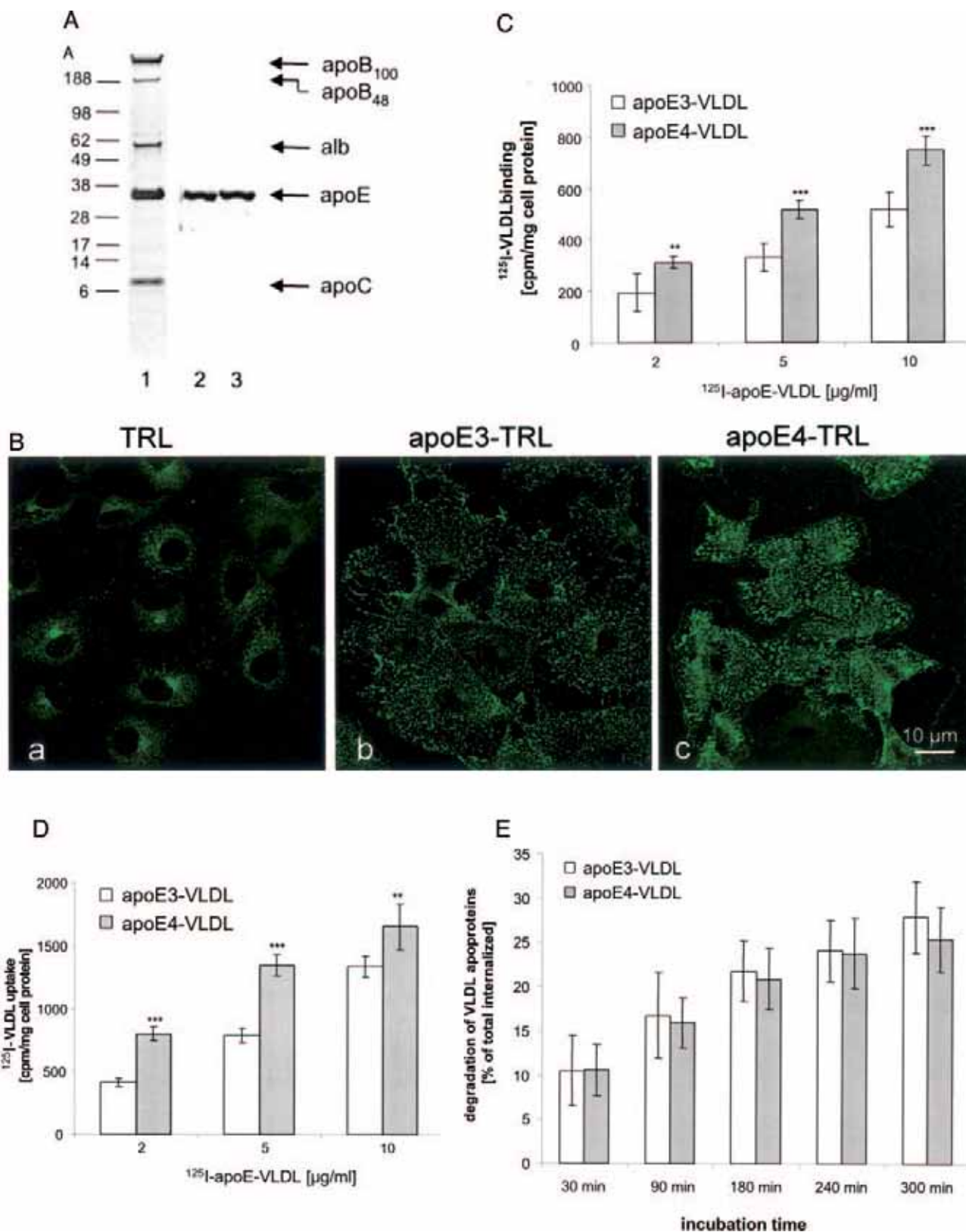


FIG. 2. Isoform-dependent cell-surface binding, internalization, and degradation of TRL and VLDL. *A*, SDS-PAGE analysis of TRL (10 μ g, lane 1), apoE3-TRL (2 μ g, lane 2), or apoE4-TRL (2 μ g, lane 3). TRL particles were delipidated and re-solubilized, and apoproteins were separated on a 4–12% gradient gel using a MES-based buffer system. Apoproteins were visualized with Coomassie Blue staining. *B*, HuH7 hepatoma cells were incubated with TRL alone (*a*) or TRL enriched with 5 μ g/ml apoE3 (*b*) or apoE4 (*c*) for 20 min at 37 °C. Cell surface-bound lipoproteins were removed with heparin, and cells were fixed in 4% paraformaldehyde and analyzed by confocal fluorescence microscopy for apoE as described above. Bar is 10 μ m. To determine cell-surface binding (*C*) and uptake (*D*), hepatoma cells were incubated with 2.5–10 μ g/ml ¹²⁵I-apoE3-VLDL and ¹²⁵I-apoE4-VLDL for 60 min at 4 or 37 °C, respectively. After washing, cells were lysed in 0.1 N NaOH and binding (4 °C) and internalized (37 °C) radioactivity was determined. Values of specific binding/uptake for ¹²⁵I-apoE3-VLDL (white bars) and ¹²⁵I-apoE4-VLDL (gray bars) are given in cpm/mg cell protein and represent the mean \pm S.D. of three independent experiments with triplicate samples. **, $p < 0.01$; ***, $p < 0.001$ by Student's *t* test. *E*, for degradation assays, HuH7 cells were incubated with 10 μ g/ml ¹²⁵I-apoE3-VLDL and ¹²⁵I-apoE4-VLDL for 60 min at 37 °C. Cells were washed at 4 °C, and cell-bound radioactive material was removed by heparin. This was followed by a second incubation

FIG. 3. TRL-derived apoE3 and apoE4 are targeted to peripheral endosomes. A, recombinant apoE3 and apoE4 were labeled with Cy3 or Cy5 and associated with TRL, respectively. Human hepatoma cells were incubated with Cy3-apoE3-TRL (2 $\mu\text{g}/\text{ml}$) and Cy5-apoE4-TRL (1 $\mu\text{g}/\text{ml}$) for 30 min at 37 °C. Cell surface-bound lipoproteins were removed with heparin, and cells were fixed in 4% paraformaldehyde. Nuclei were stained with 4',6-diamidino-2-phenylindole (blue), and sections were analyzed by confocal fluorescence microscopy for Cy3-apoE3 (a) in red and Cy5-apoE4 (b) in green. The merged image is shown in c. The arrows point to co-localized staining for apoE3 and apoE4 (a–c). Bar is 20 μm . B, HuH7 cells were incubated with 1 $\mu\text{g}/\text{ml}$ Cy3-apoE3-TRL and 1 μM LysoTracker for 0–30 min at 37 °C. Time-lapse confocal image acquisition of apoE (a) in red and lysosomal compartments (b) in green was performed at 37 °C (see “Experimental Procedures”). The merged image is shown in c. Bar is 10 μm .

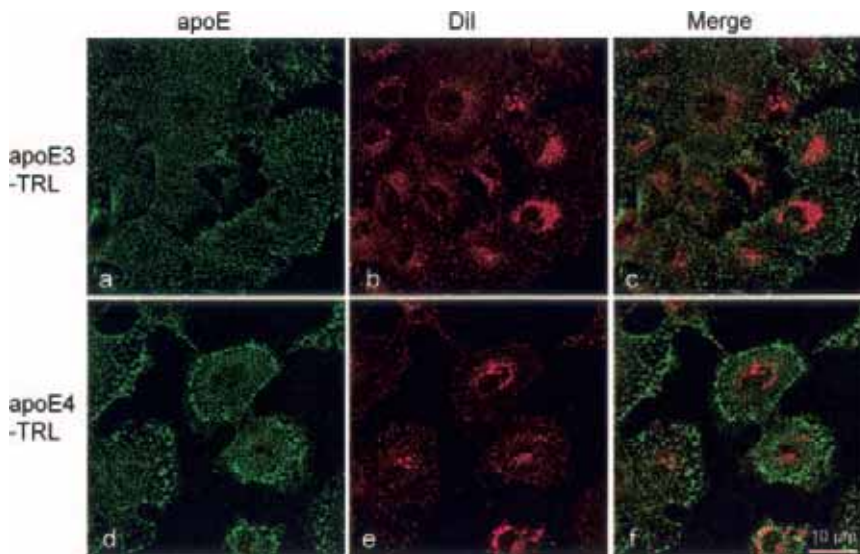
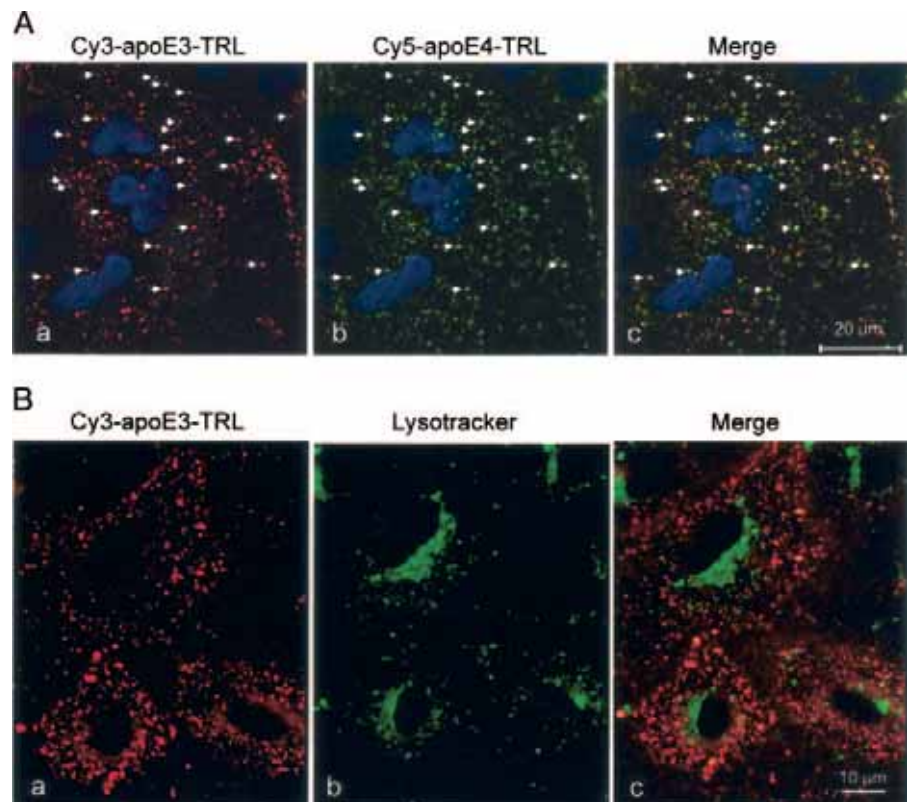


FIG. 4. Disintegration of TRL-derived apoE isoforms and phospholipids (DiI). HuH7 cells were incubated with DiI-labeled apoE3-TRL (a–c) and apoE4-TRL (d–f) for 30 min at 37 °C. After the removal of cell-bound material with heparin, cells were fixed and sections (1 μm width) were analyzed by confocal fluorescence microscopy. Cells were analyzed for apoE (a and d) in green and DiI (b and e) in red. The merged images are shown in c and f. Bar is 10 μm .

of apoE was determined (Fig. 5). First, HuH7 cells were incubated with apoE3-TRL (Fig. 5A, a and b) and apoE4-TRL (Fig. 5A, c and d) at 37 °C for 60 min, which was followed by a 60-min chase \pm HDL₃. The cells were washed with heparin, fixed, and immunostained against apoE to detect TRL-derived apoE. In the absence of HDL₃, significant amounts of internalized TRL-derived apoE3 (Fig. 5A, a) and apoE4 (Fig. 5A, c) remained intracellularly. When cells were incubated with HDL₃, only residual signals of internalized apoE3 were detectable (Fig. 5A, b). In contrast, large amounts of apoE4 were found intracellularly even in the presence of HDL₃ (Fig. 5A, d),

indicating that HDL₃-induced recycling of TRL-derived apoE4 is reduced. These findings were confirmed by apoE Western blot analysis of the chase media (Fig. 5B). No secretion of endogenous apoE was observed under these conditions (data not shown). ApoE recycling from TRL not enriched with apoE was detectable only in longer exposures (lanes 1 and 2). As determined by densitometric analysis of lanes 3–6, the HDL₃-induced recycling of apoE3 was stimulated \sim 6-fold, whereas apoE4 re-secretion was increased only 3.6-fold. In neuronal cells, it has been shown that apoE isoforms undergo different intracellular processing (41). In these experiments, internal-

at 37 °C for 30–300 min as indicated. To determine protein degradation, the media were harvested, the trichloroacetic acid-precipitable material was removed, and the content of ¹²⁵I-tyrosine in the supernatant was determined. Cells were washed and lysed in 0.1 N NaOH, and the remaining internalized radioactivity was determined. Values of specific degradation for ¹²⁵I-apoE3-VLDL (white bars) and ¹²⁵I-apoE4-VLDL (gray bars) are given as the percentage of total metabolized radioactivity and represent the mean \pm S.D. of four separate experiments with triplicate samples.

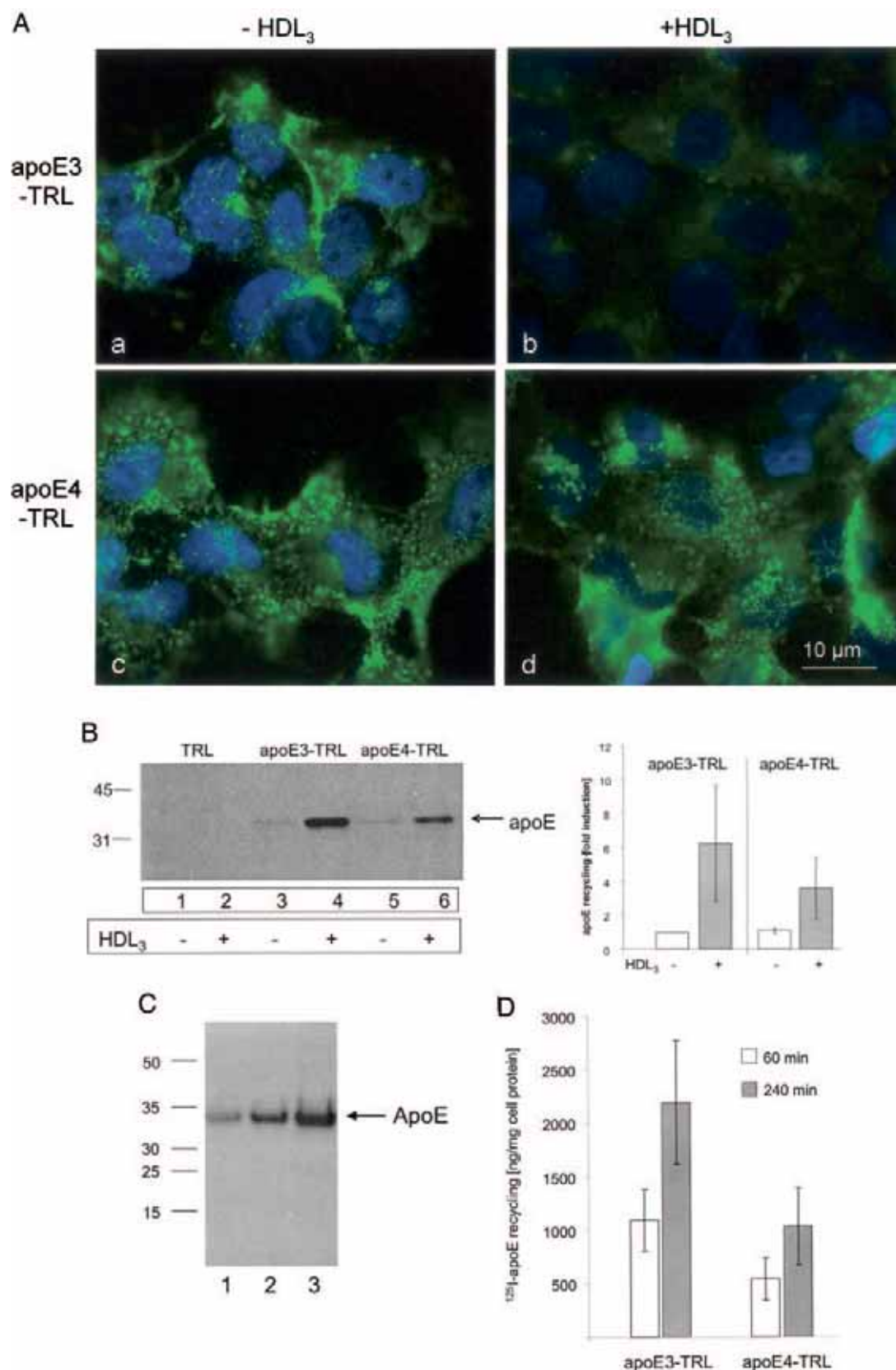


FIG. 5. HDL₃ induced recycling of TRL-derived apoE3 and apoE4. A, HuH7 cells were preincubated with apoE3-TRL (*a* and *b*) or apoE4-TRL (*c* and *d*) for 60 min at 37 °C. After removal of cell-bound material with heparin, cells were incubated ± HDL₃ (50 μg/ml) for an additional 60 min at 37 °C as indicated. The media were collected to identify recycled apoE isoforms (see Fig. 5B). Cells were fixed and analyzed by fluorescence microscopy for apoE (green). Nuclei were stained with 4',6-diamidino-2-phenylindole. Bar is 10 μm. B, pulse-chase experiments were performed by preincubating human hepatoma cells with TRL (lane 1 and 2), apoE3-TRL (lanes 3 and 4), and apoE4-TRL (lanes 5 and 6) for 60 min at 37 °C. Cell-bound material was removed with heparin, and cells were incubated ± HDL₃ (50 μg/ml) for 60 min at 37 °C as indicated. Cell culture media were harvested, and the presence of recycled intact apoE was determined by Western blot analysis (see "Experimental Procedures"). The position of apoE is indicated. Molecular mass is given in kDa. The amount of recycled apoE3 and apoE4 in the Western blot analysis was quantified by densitometry. The stimulation of HDL₃-induced apoE isoform recycling (mean ± S.D.) from three independent experiments relative to the apoE3 control (lane 3) is shown. C, HuH7 cells

ized apoE4 compared with apoE3 was more susceptible to degradation, resulting in the cellular accumulation of truncated apoE4 and formation of neurofibrillary tangle-like inclusions (41). Because increased accumulation of truncated apoE4 could contribute to the impaired recycling of apoE4, the presence of degraded apoE fragments after internalization of TRL-derived apoE was investigated (Fig. 5C). Therefore, HuH7 cells were incubated with TRL, apoE3-TRL, and apoE4-TRL for 60 min at 37 °C and cellular proteins were isolated. Similar amounts of total cell protein were separated by SDS-PAGE and analyzed by Western blot analysis using a polyclonal antibody against apoE. HuH7 cells expressed low amounts of endogenous apoE (Fig. 5C, lane 1). In agreement with the results obtained in Fig. 2, increased amounts of internalized and intact TRL-derived apoE4 (Fig. 5C, lane 3) compared with TRL-derived apoE3 (Fig. 5C, lane 2) was detected. Most importantly, the truncated apoE fragments, possibly derived from apoE degradation, were not detectable under these conditions. Thus, increased accumulation of truncated apoE4 does not contribute to the reduced recycling of apoE4.

To independently confirm impaired HDL₃-induced recycling of apoE4, pulse-chase experiments with radiolabeled apoE3-TRL and apoE4-TRL were performed. Therefore, HuH7 cells were pre-loaded with ¹²⁵I-apoE3-TRL and ¹²⁵I-apoE4-TRL and apoE recycling was determined in the presence of HDL₃, respectively (Fig. 5D). In this set of experiments, HDL₃-induced recycling of TRL-derived ¹²⁵I-apoE3 was increased ~2-fold at *t* = 60 and 240 min compared with ¹²⁵I-apoE4.

Previously, we have demonstrated that apoE recycling is associated with cholesterol efflux (13). To analyze the effect of TRL-derived apoE isoforms on cholesterol efflux, human hepatoma cells were labeled overnight with ³H-cholesterol and loaded with apoE3-TRL or apoE4-TRL (Fig. 6). Surface-bound lipoproteins were removed by heparin, and HDL₃-induced cholesterol efflux was determined after 60 and 240 min. Similar to the results obtained in the apoE recycling studies (Fig. 5), cholesterol efflux from apoE3-TRL pre-incubated cells was increased 2.5–3.0-fold at *t* = 60 and 240 min compared with apoE4-TRL-loaded cells. In summary, reduced apoE4 recycling correlated with decreased HDL-induced cholesterol efflux.

HDL-induced ApoE Recycling Is Independent of ABCA1 Activity—Cellular cholesterol efflux is known to be critically dependent upon ABCA1 activity (42, 43). Because lipid-free apoA-I and HDL₃-induced apoE recycling is associated with cholesterol efflux (13, 14), we investigated the possible role of ABCA1 for apoE recycling. Therefore, pulse-chase experiments with normal fibroblasts and ABCA1-deficient Tangier fibroblasts were performed. The recycling of TRL-derived apoproteins in fibroblasts is comparable with the results obtained from hepatoma cells (9, 10). Cells were incubated with ¹²⁵I-TRL for 60 min at 37 °C. Under these conditions, similar amounts of the ¹²⁵I-TRL protein were found in normal (21.8 ± 2.2 ng/mg cell protein) and Tangier fibroblasts (22.5 ± 2.0 ng/mg cell protein). The cells then were washed with heparin, and apoE recycling was analyzed in the presence or absence of HDL₃ and lipid-free apoA-I (Fig. 7A). An ~2-fold induction of HDL₃ and apoA-I induced recycling of ¹²⁵I-TRL apoproteins was determined for both normal and Tangier fibroblasts. In this set of experiments, apoA-I-induced recycling in Tangier fibroblasts

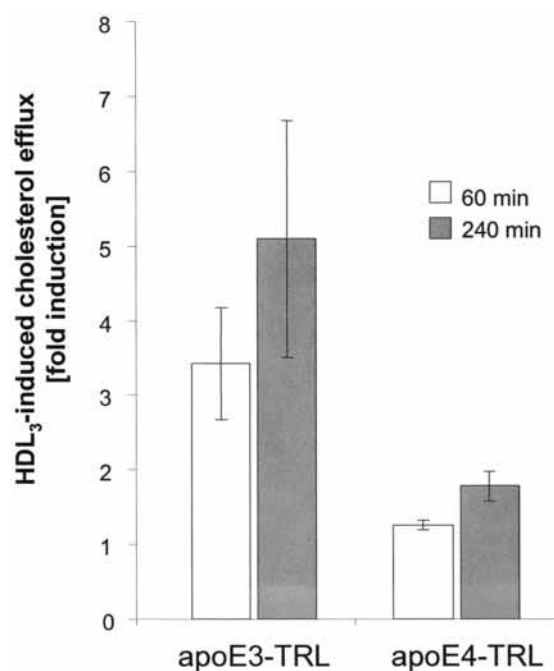


FIG. 6. Recycling of apoE4 is associated with reduced efflux of cellular cholesterol. Human hepatoma cells were pre-loaded with ³H-cholesterol (100,000 cpm/ml) for 24 h at 37 °C. Cells were washed with PBS and incubated in the presence or absence of TRL, apoE3-TRL, and apoE4-TRL for 60 min at 37 °C. Cells were washed with heparin and incubated for an additional 60 (white bar) and 240 min (gray bar) at 37 °C with media in the presence or absence of 50 µg/ml HDL₃. Aliquots of the media were harvested to determine ³H-cholesterol efflux and were normalized to total cellular protein. The values of ³H-cholesterol efflux represent the ratio of ±HDL-incubated cells and are given relative to the fold-induction of efflux in TRL-incubated samples at *t* = 60 min. The mean ± S.D. of four independent experiments with triplicates is shown.

was slightly, but not significantly, reduced compared with the controls.

To investigate the possible involvement of ABCA1 in apoE recycling in hepatoma cells, ABCA1 expression was induced in HuH7 cells and apoE recycling was determined. Overnight treatment of cells with LXR/RXR agonists (OH-Chol + RA) resulted in a 1.6-fold induction of ABCA1 expression as judged by real-time PCR (Fig. 7B). To analyze apoE recycling, hepatoma cells were treated ± OH-Chol/RA, loaded with ¹²⁵I-TRL for 60 min at 37 °C, and then washed with heparin. Because ABCA1 activity assays are best performed at 4–20 h (42, 44), apoE recycling was measured in the absence or presence of HDL₃ or apoA-I after 240 min (Fig. 7C). In these experiments, HDL₃- and apoA-I-induced recycling of TRL apoproteins was similar in control and ABCA1-induced cells. Similar to studies in macrophages (38, 42), apoA-I significantly induced cholesterol efflux under these conditions in HuH7 cells (*p* = 0.001, data not shown). Taken together, our findings suggest that ABCA1 is not involved in the recycling of TRL-derived apoE.

DISCUSSION

The aim of this study was to compare the effect of the apoE isoforms on the intracellular processing of TRL components. Dis-

were incubated with TRL (lane 1), apoE3-TRL (lane 2), or apoE4-TRL (lane 3) for 60 min at 37 °C. After removal of cell-bound material with heparin, cell proteins were isolated and 5 µg of cell protein/lane were separated by 4–12% SDS-PAGE and analyzed by Western blot for apoE. Molecular mass markers in kDa are given. D, pulse-chase experiments were performed by incubating HuH7 hepatoma cells with ¹²⁵I-apoE3-TRL or ¹²⁵I-apoE4-TRL for 60 min at 37 °C. Cells were washed with heparin and incubated for an additional 60 (white bar) and 240 min (gray bar) at 37 °C with media in the presence or absence of 50 µg/ml HDL₃ as indicated. The media were harvested, and the amount of re-secreted ¹²⁵I-apoE3 and ¹²⁵I-apoE4 was determined. The remaining cells were lysed, and protein content was determined. The radioactivity is given (cpm/mg cell protein) and represents the mean ± S.D. of four independent experiments with triplicate samples.

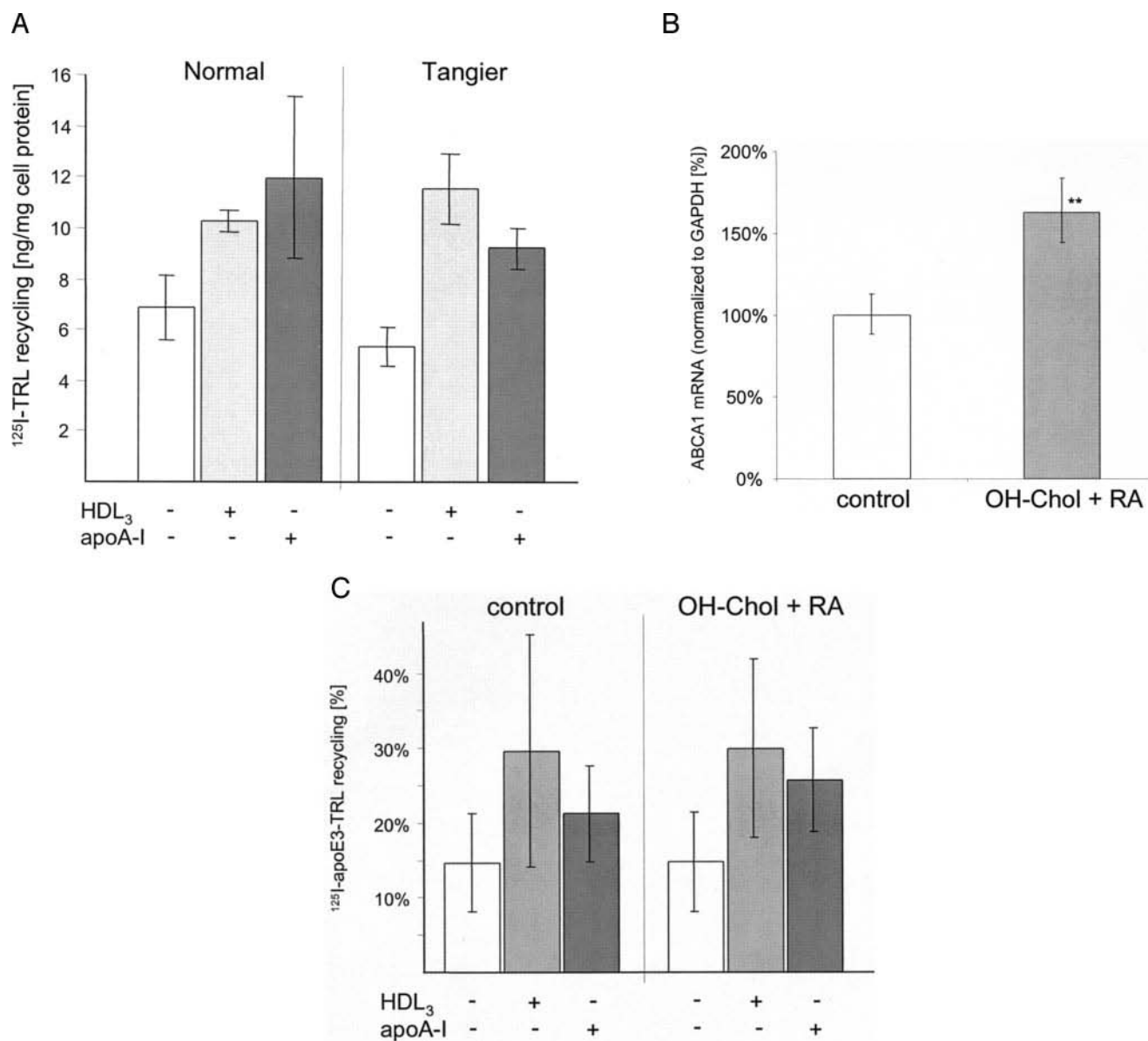


FIG. 7. Intracellular processing of TRL-associated proteins in normal and Tangier fibroblasts. *A*, normal and Tangier human fibroblasts were incubated with ^{125}I -TRL for 60 min at 37 °C (see “Experimental Procedures”). Cells were washed at 4 °C, and cell-bound material was removed by heparin. After incubation for additional 90 min with or without HDL₃ (50 $\mu\text{g}/\text{ml}$) at 37 °C as indicated, the media were collected to determine recycled ^{125}I -TRL proteins. The remaining cells were lysed as described above. The data are given in ng/mg cell protein and represent the mean \pm S.D. of three independent experiments with duplicate samples. *B*, human hepatoma cells were incubated with or without (*control*) 5 mM OH-Chol and 5 mM RA for 24 h as indicated. Cells were harvested, and total RNA was isolated. ABCA1 expression was determined using quantitative reverse transcriptase-PCR and normalized to GAPDH mRNA levels as described under “Experimental Procedures.” Expression levels are given in percent relative to the control. Each *bar* represents the mean of three experiments \pm S.D. (**, $p < 0.01$). *C*, human hepatoma cells were preincubated as in *B*. The cells then were incubated with ^{125}I -TRL for 60 min at 37 °C and washed with heparin to remove cell-bound material. After incubation for an additional 90 min \pm HDL₃ (50 $\mu\text{g}/\text{ml}$) at 37 °C, degraded and recycled ^{125}I -TRL proteins in the media and remaining radioactivity in the cells were determined as described previously (9). The percentage of recycled ^{125}I -TRL proteins was calculated and represents the mean \pm S.D. of three independent experiments with duplicate samples.

integration of internalized TRL resulted in the re-secretion of TRL-derived apoE (9–11, 45), a process that is stimulated by extracellular apoA-I or HDL (13, 14) and is associated with cholesterol efflux (13). However, little is known regarding the potential differences in the intracellular processing related to the apoE isoforms, which could possibly help to explain the effects of apoE3 and apoE4 on lipoprotein metabolism. Here, we demonstrated that HDL-induced recycling of TRL-derived apoE4 is impaired in comparison to apoE3. The reduced recycling of apoE4 was associated with a decreased cholesterol efflux, suggesting that the isoform-specific intracellular trafficking affects cholesterol transport to the plasma membrane and consequently modulates the composition of secreted lipoproteins.

Initial experiments in this study demonstrated an elevated cell-surface binding and uptake of apoE4-containing VLDL and TRL into human hepatoma cells compared with apoE3, whereas the relative amount of degraded apoproteins was similar between the isoforms (Figs. 2 and 3). These findings are in agreement with the studies that described an increased internalization of apoE4-containing VLDL (24, 25). In these studies, the authors hypothesized that the higher binding affinity of apoE4 to the LDL receptor could be responsible for the increased internalization of apoE4 containing VLDL particles. The increased uptake of apoE4-TRL mediated by hepatic lipoprotein receptors could be responsible for the pathological lipoprotein profile in apoE4 individuals. It has been proposed

that increased TRL uptake leads to an intracellular accumulation of cholesterol. This could ultimately down-regulate hepatic LDL receptor expression (26) and thereby increase LDL plasma levels, which are associated with an increased risk for atherosclerosis (20). However, apoE4-induced down-regulation of the LDL receptor alone cannot explain the striking differences between apoE3 and apoE4 in the development of atherosclerosis (46). Malloy *et al.* (46) hypothesized that, in hepatocytes, TRL-derived apoE4 might be trapped after LDL receptor-mediated endocytosis, thus reducing its availability for the transfer to nascent lipoproteins. Our results confirmed this hypothesis, because apoE4, but not apoE3, accumulates in hepatoma cells (Figs. 2B and 4) and is not recycled (see below) from peripheral endosomal compartments.

We and others (13, 14) have demonstrated that extracellular HDL₃ and apoA-I induce the recycling of internalized TRL-derived apoE. This process is associated with the concomitant efflux of cellular cholesterol and modulates the composition of HDL in hepatoma cells and macrophages (13). In this study, the stimulatory effect of HDL₃ on apoE recycling was observed only for TRL-derived apoE3 but not for apoE4 (Fig. 5). Furthermore, no obvious differences between the intracellular degradation of TRL-derived apoE4 and apoE3 could be detected in hepatoma cells (Fig. 5C). Thus, the lack of truncated apoE fragments suggested that full-length apoE4 accumulates intracellularly and is not transferred efficiently to HDL during the recycling process. This mechanism may contribute to the reduced amounts of apoE4, as compared with apoE3, on HDL in mice and men (20, 26, 30–32). Several lipoprotein receptors, such as low-density lipoprotein receptor and low-density lipoprotein receptor-related protein, can mediate the internalization of lipoproteins via interaction with apoE. However, it has been demonstrated that none of the above receptors alone is responsible for apoE recycling (47). Rather, the different biophysical characteristics of apoE3 and apoE4 could provide an alternative explanation for the differential intracellular routing of the apoE isoforms. Accordingly, apoE4 has a greater propensity than apoE3 to form a molten globule at a low pH (48), which correlates with the increased lipid-binding properties of apoE4 compared with apoE3 (49). In the context of HDL-induced apoE recycling, the drop in the pH after acidification in early endosomal compartments may therefore lead to a conformational change of internalized apoE4 but not that of apoE3. The enhanced exposure of hydrophobic residues of apoE4 could alter the binding to lipoprotein receptors or lead to an increased association with endosomal membranes or result in an apoE4 self-aggregation, ultimately inhibiting an efficient transfer of apoE4 to lipid-poor HDL particles during recycling. Future experiments will have to clarify whether different intracellular trafficking of lipoprotein receptors or the specific biochemical characteristics of apoE4 determine the abnormal intracellular sorting of this apoE isoform. Furthermore, analogous studies with apoE2, which is known for its defective binding to the low-density lipoprotein receptor, will be an important issue to further dissect the isoform-specific intracellular pathways.

The critical role of apoE in the formation of apoE-containing HDL and the pathogenesis of atherosclerosis seems to be closely linked to the activity of ABCA1, one of the major regulators of cholesterol efflux (for reviews see Refs. 50–52). Therefore, several studies investigated the impact of apoE isoforms on ABCA1-dependent efflux and recent findings from Remaley *et al.* (53) demonstrated that exogenous apoE stimulates cholesterol efflux via ABCA1 in macrophages. Vice versa, ABCA1 participates in the regulation of intracellular apoE transport. The induction of ABCA1 activity promotes the secretion of

endogenous apoE (54), and exogenous apoA-I facilitates the secretion and the recycling of apoE in macrophages (14, 55). These findings indicated that ABCA1 could be involved in the regulation of HDL-induced apoE recycling in hepatocytes. However, we were unable to identify a potential link between apoE recycling and ABCA1 expression (Fig. 7). This might be explained by the fact that ABCA1-mediated effects on apoE secretion have been measured after 4–16 h (44, 55), whereas HDL-induced apoE recycling was completed within 60 min (13, 14). Therefore, we conclude that the isoform-specific apoE-recycling pathway, which is responsible for apoE and cholesterol enrichment of HDL particles during the postprandial state, is independent of ABCA1.

In summary, we could demonstrate for the first time that the HDL-induced recycling of TRL-derived apoE is isoform-specific. ApoE3 recycling is associated with concomitant cholesterol efflux and thereby contributes to the formation of apoE-containing HDL, whereas apoE4 accumulates within endosomal compartments and is connected to an impaired cholesterol efflux. Although the implications of impaired apoE4 recycling for HDL metabolism *in vivo* are yet unclear, it could contribute to the low apoE4 and cholesterol content on HDL particles in apoE4 subjects (20, 26, 30–32). Further *in vivo* studies in animal models are necessary to understand whether isoform-specific differences in apoE recycling could determine the variation of plasma lipoprotein profiles among carriers with different apoE isoforms.

Acknowledgments—We thank H. B. Brewer, Jr. (National Institutes of Health, Bethesda, Maryland) for providing fibroblasts from Tangier patients. We are grateful to A. Rosche and S. Ehret for excellent technical assistance and E. Kahraman, M. Steinwaerder, and B. Kratzert for performing parts of the experiments.

REFERENCES

- Mahley, R. W., and Ji, Z. S. (1999) *J. Lipid Res.* **40**, 1–16
- Goldberg, I. J., and Merkel, M. (2001) *Front Biosci.* **6**, D388–D405
- Beisiegel, U., Weber, W., Ihrke, G., Herz, J., and Stanley, K. K. (1989) *Nature* **341**, 162–164
- Beisiegel, U., Weber, W., and Bengtsson-Olivecrona, G. (1991) *Proc. Natl. Acad. Sci. U. S. A.* **88**, 8342–8346
- Heeren, J., Niemeier, A., Merkel, M., and Beisiegel, U. (2002) *J. Mol. Med.* **80**, 576–584
- Zhang, S. H., Reddick, R. L., Piedrahita, J. A., and Maeda, N. (1992) *Science* **258**, 468–471
- Rohlmann, A., Gotthardt, M., Hammer, R. E., and Herz, J. (1998) *J. Clin. Investig.* **101**, 689–695
- Tabas, I., Lim, S., Xu, X. X., and Maxfield, F. R. (1990) *J. Cell Biol.* **111**, 929–940
- Heeren, J., Weber, W., and Beisiegel, U. (1999) *J. Cell Sci.* **112**, 349–359
- Heeren, J., Grewal, T., Jackle, S., and Beisiegel, U. (2001) *J. Biol. Chem.* **276**, 42333–42338
- Fazio, S., Linton, M. F., Hasty, A. H., and Swift, L. L. (1999) *J. Biol. Chem.* **274**, 8247–8253
- Rensen, P. C., Jong, M. C., van Vark, L. C., van der, B. H., Hendriks, W. L., Van Berkel, T. J., Biessen, E. A., and Havekes, L. M. (2000) *J. Biol. Chem.* **275**, 8564–8571
- Heeren, J., Grewal, T., Laatsch, A., Rottke, D., Rinninger, F., Enrich, C., and Beisiegel, U. (2003) *J. Biol. Chem.* **278**, 14370–14378
- Farkas, M. H., Swift, L. L., Hasty, A. H., Linton, M. F., and Fazio, S. (2003) *J. Biol. Chem.* **278**, 9412–9417
- Huang, Y., von Eckardstein, A., Wu, S., Maeda, N., and Assmann, G. (1994) *Proc. Natl. Acad. Sci. U. S. A.* **91**, 1834–1838
- Cullen, P., Cignarella, A., Brennhansen, B., Mohr, S., Assmann, G., and von Eckardstein, A. (1998) *J. Clin. Investig.* **101**, 1670–1677
- Lin, C. Y., Duan, H., and Mazzone, T. (1999) *J. Lipid Res.* **40**, 1618–1627
- Kuipers, F., Jong, M. C., Lin, Y., Eck, M., Havinga, R., Bloks, V., Verkade, H. J., Hofker, M. H., Moshage, H., Berkel, T. J., Vonk, R. J., and Havekes, L. M. (1997) *J. Clin. Investig.* **100**, 2915–2922
- Huang, Y., Liu, X. Q., Rall, S. C., Jr., Taylor, J. M., von Eckardstein, A., Assmann, G., and Mahley, R. W. (1998) *J. Biol. Chem.* **273**, 26388–26393
- Davignon, J., Gregg, R. E., and Sing, C. F. (1988) *Arteriosclerosis* **8**, 1–21
- Roses, A. D. (1996) *Annu. Rev. Med.* **47**, 387–400
- Schneider, W. J., Kovanen, P. T., Brown, M. S., Goldstein, J. L., Utermann, G., Weber, W., Havel, R. J., Kotite, L., Kane, J. P., Innerarity, T. L., and Mahley, R. W. (1981) *J. Clin. Investig.* **68**, 1075–1085
- Mahley, R. W. (1988) *Science* **240**, 622–630
- Bohnet, K., Pillot, T., Visvikis, S., Sabolovic, N., and Siest, G. (1996) *J. Lipid Res.* **37**, 1316–1324
- Mamotte, C. D., Sturm, M., Foo, J. I., van Bockxmeer, F. M., and Taylor, R. R. (1999) *Am. J. Physiol.* **276**, E553–E557

26. Gregg, R. E., Zech, L. A., Schaefer, E. J., Stark, D., Wilson, D., and Brewer, H. B., Jr. (1986) *J. Clin. Investig.* **78**, 815–821
27. Knouff, C., Hinsdale, M. E., Mezdour, H., Altenburg, M. K., Watanabe, M., Quarfordt, S. H., Sullivan, P. M., and Maeda, N. (1999) *J. Clin. Investig.* **103**, 1579–1586
28. Huang, Y., von Eckardstein, A., Wu, S., and Assmann, G. (1995) *J. Clin. Investig.* **96**, 2693–2701
29. Michikawa, M., Fan, Q. W., Isobe, I., and Yanagisawa, K. (2000) *J. Neurochem.* **74**, 1008–1016
30. Weisgraber, K. H. (1990) *J. Lipid Res.* **31**, 1503–1511
31. Dallongeville, J., Lussier-Cacan, S., and Davignon, J. (1992) *J. Lipid Res.* **33**, 447–454
32. Hopkins, P. C., Huang, Y., McGuire, J. G., and Pitas, R. E. (2002) *J. Lipid Res.* **43**, 1881–1889
33. Remaley, A. T., Schumacher, U. K., Stonik, J. A., Farsi, B. D., Nazih, H., and Brewer, H. B., Jr. (1997) *Arterioscler. Thromb. Vasc. Biol.* **17**, 1813–1821
34. Rinninger, F., Brundert, M., Jackle, S., Galle, P. R., Busch, C., Izbicki, J. R., Rogiers, X., Henne-Bruns, D., Kremer, B., and Broelsch, C. E. (1994) *Hepatology* **19**, 1100–1114
35. Mann, W. A., Meyer, N., Berg, D., Greten, H., and Beisiegel, U. (1999) *Atherosclerosis* **145**, 61–69
36. Morrow, J. A., Arnold, K. S., and Weisgraber, K. H. (1999) *Protein Expression Purif.* **16**, 224–230
37. Goldstein, J. L., Basu, S. K., and Brown, M. S. (1983) *Methods Enzymol.* **98**, 241–260
38. Costet, P., Luo, Y., Wang, N., and Tall, A. R. (2000) *J. Biol. Chem.* **275**, 28240–28245
39. Laatsch, A., Ragozin, S., Grewal, T., Beisiegel, U., and Heeren, J. (2004) *Eur. J. Cell Biol.* **83**, 113–120
40. Wang, N., Lan, D., Chen, W., Matsuura, F., and Tall, A. R. (2004) *Proc. Natl. Acad. Sci. U. S. A.* **101**, 9774–9779
41. Huang, Y., Liu, X. Q., Wyss-Coray, T., Brecht, W. J., Sanan, D. A., and Mahley, R. W. (2001) *Proc. Natl. Acad. Sci. U. S. A.* **98**, 8838–8843
42. Wang, N., Silver, D. L., Costet, P., and Tall, A. R. (2000) *J. Biol. Chem.* **275**, 33053–33058
43. Oram, J. F., Lawn, R. M., Garvin, M. R., and Wade, D. P. (2000) *J. Biol. Chem.* **275**, 34508–34511
44. Krimbou, L., Denis, M., Haidar, B., Carrier, M., Marcil, M., and Genest, J., Jr. (2004) *J. Lipid Res.* **45**, 839–848
45. Swift, L. L., Farkas, M. H., Major, A. S., Valyi-Nagy, K., Linton, M. F., and Fazio, S. (2001) *J. Biol. Chem.* **276**, 22965–22970
46. Malloy, S. I., Altenburg, M. K., Knouff, C., Lanningham-Foster, L., Parks, J. S., and Maeda, N. (2004) *Arterioscler. Thromb. Vasc. Biol.* **24**, 91–97
47. Farkas, M. H., Weisgraber, K. H., Shepherd, V. L., Linton, M. F., Fazio, S., and Swift, L. L. (2004) *J. Lipid Res.* **45**, 1546–1554
48. Morrow, J. A., Hatters, D. M., Lu, B., Hochtl, P., Oberg, K. A., Rupp, B., and Weisgraber, K. H. (2002) *J. Biol. Chem.* **277**, 50380–50385
49. Saito, H., Dhanasekaran, P., Baldwin, F., Weisgraber, K. H., Phillips, M. C., and Lund-Katz, S. (2003) *J. Biol. Chem.* **278**, 40723–40729
50. von Eckardstein, A., Nofer, J. R., and Assmann, G. (2001) *Arterioscler. Thromb. Vasc. Biol.* **21**, 13–27
51. Curtiss, L. K., and Boisvert, W. A. (2000) *Curr. Opin. Lipidol.* **11**, 243–251
52. Oram, J. F. (2003) *Arterioscler. Thromb. Vasc. Biol.* **23**, 720–727
53. Remaley, A. T., Stonik, J. A., Demosky, S. J., Neufeld, E. B., Bocharov, A. V., Vishnyakova, T. G., Eggerman, T. L., Patterson, A. P., Duverger, N. J., Santamarina-Fojo, S., and Brewer, H. B., Jr. (2001) *Biochem. Biophys. Res. Commun.* **280**, 818–823
54. von Eckardstein, A., Langer, C., Engel, T., Schaukal, I., Cignarella, A., Reinhardt, J., Lorkowski, S., Li, Z., Zhou, X., Cullen, P., and Assmann, G. (2001) *FASEB J.* **15**, 1555–1561
55. Rees, D., Sloane, T., Jessup, W., Dean, R. T., and Kritharides, L. (1999) *J. Biol. Chem.* **274**, 27925–27933